Original Article

Secondhand Smoke Sequelae on The Lungs of Male Albino Rats During Childhood and Adulthood Periods with Special References to Bronchiolar and Alveolar Cells

Abeer Ibraheem Omar, Eman Abas Farag and Marwa Mohamed Yousry

Department of Histology, Faculty of Medicine, Cairo University, Cairo, Egypt

ABSTRACT

Introduction: Tobacco smoking is one of the principal epidemics, a major predisposing factor for multiple non-communicable diseases as vascular, cardiac and respiratory diseases and the 2nd major death risk factor. Passive tobacco smoke inhalation, known as secondhand smoke (SHS) or environmental tobacco smoke, is more common in the closed environment (indoor exposure). This type of smoke inhalation causes 15% of smoking-induced deaths and 2% of total deaths. So, smoking in closed public areas is banned in many countries. In low & middle socio-economic countries, children -at their homes- are the most age group at risk of SHS exposure.

Aim of the Work: This study aimed at evaluating and comparing the possible hazardous effects of SHS on the lungs of male albino rats in childhood and adulthood periods with highlighting the consequences on the bronchiolar ciliated & Clara cells and alveolar pneumocytes-I & II.

Materials and Methods: 24 male albino rats were chosen and sorted equally into child group (~21 days, group I) and adult group (~90 days, group II). Each group was subdivided equally into 2 subgroups: sham-exposed (exposed to fresh air, two times daily with 6 hours interval) and smoke-exposed (treated as sham-exposed subgroup but with SHS instead of fresh air). After 2 weeks, just before sacrifice, serum cotinine level was measured for all animals. Biochemical, histological, immunohistochemical [for Clara cells secretory protein (CCSP), surfactant protein-C (SP-C), ß-tubulin, caspase-3 & CD-68] and morphometric studies were done.

Results: Smoke-exposed subgroups (child & adult) showed lung inflammatory signs and degenerative changes in bronchiolar ciliated and Clara cells and in pneumocytes-I & II that were more noticeable in child subgroup.

Conclusion: SHS has severe detrimental effects on structure and function of rats' lungs via oxidative, inflammatory & apoptotic mechanisms. Additionally, children are more vulnerable than adults to these damaging effects.

Received: 16 July 2022, **Accepted:** 26 September 2022

Key Words: ß-tubulin, CCSP, child rat, SHS, SP-C.

Corresponding Author: Abeer Ibraheem Omar, MD, Department of Histology, Faculty of Medicine, Cairo University, Cairo, Egypt, **Tel.**: +20 10 0259 6677, **E-mail:** kaboree2002@gmail.com

ISSN: 1110-0559, Vol. 46, No. 4

INTRODUCTION

Tobacco smoking is the most prominent triggering cause of multiple non-communicable diseases such as vascular and ischemic heart diseases, respiratory diseases as chronic obstructive pulmonary disease (COPD), compromised bone quality and bone healing, stroke, and cancers especially lung cancer[1,2]. It is considered as one of the biggest world epidemics and the 2nd risk factor for death[3] where it is responsible for about 100 million deaths in the 20th century[2]. Additionally, it is predicted to cause 1 billion deaths in the 21st century[4]. These deaths represent about 20% of male deaths and 5% of female deaths above 30 years[2] and 15% of the total deaths worldwide[3]. Smoking- induced death is described as premature death[5] as 50-70% of these deaths occur in the middle age[2].

Tobacco smoke is generated by two different ways[6]. The first way occurs when the tobacco is burnt at a high temperature then passes through the tobacco column and the cigarette filter under the effect of its active inhalation by the smokers. In this case the smoke is called mainstream (central) smoke. The second way results from tobacco burning at a lower temperature throughout the gradual and spontaneous flaming of any form of tobacco smoking (cigarette, cigar, or pipe). Through this way the generated smoke is named side-stream (peripheral) smoke. This type of smoke is more toxic than the mainstream smoke where it is documented to have higher levels of certain toxins as carboxyhemoglobin and nicotine. So, its inhalation causes 4 times more harmfulness and its deposition on skin leads to 3 times more toxicity and 2-6 times more carcinogenicity than mainstream smoke[7].

Such smoke enters the body through the respiratory system via inhalation into the lungs. Then it passes through the pulmonary blood vessels to the different body systems and organs where it alters their metabolic functions leading to the serious hazardous effects[8].

The tobacco smoke inhalation is either active or passive. In case of active smoking, the smoke is actively inhaled by the smoker who will be exposed to both mainstream and side-stream smoke. However, in case of passive smoking,

Personal non-commercial use only. EJH copyright © 2023. All rights served *DOI: 10.21608/ejh.2022.150492.1725*

the non-smoker is passively exposed to the environment polluted by what is called secondhand smoke (SHS) or environmental tobacco smoke (ETS), especially in the closed environment (indoor exposure). Such type of smoke includes the side-stream smoke (smoke of cigarette smoldering) and the mainstream smoke (the smoke exhaled by the active smoker)[1].

Thirdhand smoke (THS) is another type of smoke to which the non-smokers are exposed. THS is not a direct smoke, but residues of SHS that accumulate and contaminate the surroundings (walls, floors, curtains, fur of animals and any other surfaces) then discharged back to the air[9].

Secondhand smoke accounts for 15% of the smoking-triggered deaths and 2% of the total global deaths (more than deaths from road accidents)[3]. Thus, in some countries, smoking is banned in the public closed areas such as workplaces, shops, supermarkets, ways of transportation, airports, cinemas, theaters, etc. to protect the non-smokers from being chronically exposed to SHS and its hazards[10].

The children at home, especially in the countries with low & middle socio-economic status, are the most vulnerable age group to such exposure. In 20 low-middle socio-economic countries 36% (in Egypt) to 90% (in Mexico) of children are living with at least one adult smoker and exposed to SHS. This exposure occurs due to the insufficient control of smoking at homes[11] and the widespread of smoking among children's parents and guardians (33% of total men and 6% of total women are smokers[12]).

This study aimed at assessing and comparing the possible hazardous effects of SHS on the lungs of male albino rats in childhood and adulthood stages of life with highlighting the effects on the bronchiolar ciliated & Clara cells and alveolar pneumocytes-I & II.

MATERIALS AND METHODS

Experimental Design

Sixteen male albino rats [at ~P21 (P represents postnatal day), the rats were in the childhood stage] together with another sixteen rats aged ~90 days [the rats were mature adults] were housed in the laboratory animal house unit, Faculty of Medicine, Cairo University according to the guidelines stated by Cairo University-Institutional Animal Care and Use Committee (CU-IACUC) [approval number CU/III/F/55/20]. They were subjected to the same environmental circumstances for 2 days before starting the experiment to acclimatize to the new surrounding environment. They were kept at 24 ± 1°C in normal light/dark cycle and offered ordinary chow and water ad libitum. During the whole experimental duration, the animals were separated in two main groups which were kept in the same previous environmental conditions:

Pilot study was done to check the tolerability of rats to smoke exposure as follows

Two child rats were subjected to SHS (mainstream & side-stream) two times daily (at 9 a.m. and 3 p.m. with six hours interval). Each time, they were exposed to SHS of two cigarettes (10 min each)[1]. Another two child rats were used as child control and exposed to fresh air instead of smoke, in the designed apparatus following the same schedule.

Two adult rats were exposed to SHS and treated as child rats and another two were used as adult control as in case of child control.

During SHS exposure, exactly with the beginning of the 2nd cigarette at each exposure time, the child and the adult rats showed marked decrease in their activity together with signs of respiratory distress (dyspnea, rapid shallow breathing, gasping and abdominal effort in breathing). So, the exposure was stopped, and the procedure was repeated with one cigarette at each exposure time (at 9 a.m. and another one at 3 p.m.).

The experimental study

Group I (child group, 12 rats): The rats were equally divided into two subgroups:

- Subgroup Ia (child/sham-exposed subgroup, 6 rats): The rats of this group were considered as the control rats for childhood stage. They were subjected to the same procedure of the smoke exposure as in subgroup Ib, but with fresh air instead of SHS. This occurred two times daily (at 9 a.m. and 3 p.m. with six hours interval) for two weeks.
- Subgroup Ib (child/smoke-exposed subgroup, 6 rats): The rats were exposed, for two weeks[13], to SHS (mainstream & side-stream) of one cigarette in the morning (9 a.m.) and one cigarette in the afternoon (3 p.m.) with six hours interval. This occurred for 10 min each time (till the end of the cigarette burning)[13].

Group II (adult group, 12 rats): The rats were equally divided into two subgroups:

- Subgroup IIa (adult/sham-exposed subgroup, 6 rats): This subgroup's animals were considered as control for adult rats. They were treated as animals of subgroup Ia.
- Subgroup IIb (adult/smoke-exposed subgroup, 6 rats): The animals of this subgroup were exposed to SHS as those of subgroup Ib.

Secondhand smoke exposure

The apparatus used

The rats were exposed to SHS using the apparatus utilized previously[13] after being modified to permit animal exposure to both mainstream and side-stream smokes. The modified apparatus was formed of (Figure 1):

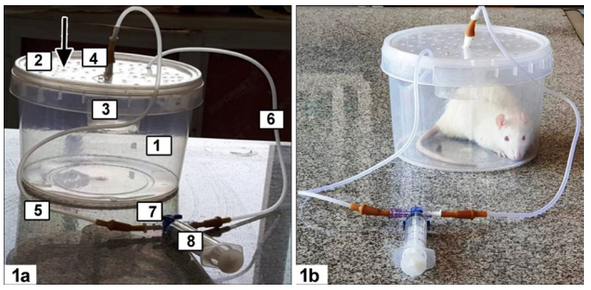

Fig. 1: Photos for the secondhand smoke apparatus illustrating: **1a:** The apparatus' components [inhalation chamber (1), lid (2) with multiple holes (arrow), ash container (3), a cigarette (4), tube A (5), tube B (6), three-way stopcock (7) & a 20 cc syringe (8)]. **1b:** The apparatus with an adult rat inside it just before the beginning of smoke exposure.

- A transparent plastic container (inhalation chamber), cylindrical in shape (10 cm radius, 20 cm height) to ensure homogenous exposure to smoke. The cylinder had a lid with multiple holes to mimic the indoor environment and avoid rat's asphyxia.
- A small plastic transparent cylinder for cigarette ash deposition was fixed into the inhalation cylinder's lid. This ash container prevented THS exposure where it prevented the deposition of the ash on the rat's fur and skin and its ingestion when the rat licked itself.
- A cigarette [an ordinary-sized cigarette with a filter (Marlboro; Philip Morris International, Santa Cruz, RS, Brazil)]. Each cigarette, according to the product label, has 10 mg carbon monoxide, 10 mg tar and 0.8 mg nicotine.
- A medical conducting tubing (Deltalab 4x6 mm Medical Grade Silicone Tubing, medline scientific, product code: 350046).
- Three-way stopcock (Flow Art Needle Free Connector with Three Way Stopcock Wide Bore, StarkMed, product code: FLO-ATUWB3010, Australia).
- A 20-cc syringe (Home Science Tools, USA).

Two conducting silicone tubing (tube A & tube B, 0.5 m each) were cut from the medical conducting tubing and fixed to the three-way stopcock that was connected to the syringe. The cigarette was fixed to the free end of tube A and placed inside the ash cylinder. The open end of tube B was positioned through one of the holes of the inhalation cylinder's cover away from the ash container. All the connections were sealed and air-tight to prevent the smoke escape.

The Rats exposure at the laboratory animal house unit

To ensure that all rats received the same amount of smoke:

First, one rat was put in the inhalation chamber at a time, as when the rats are in groups, they prefer to get together covering each other, so the smoke might be unequally distributed.

Second, all the plastic and the rubber components of the apparatus were washed thoroughly with distilled water and dried with fresh air in-between rats to remove the accumulated smoke residues avoiding THS exposure.

The cigarette was lit (to allow side-stream smoke exposure through cigarette smoldering). To simulate the mainstream smoke, the three-way stopcock was adjusted to open the line between the syringe and tube A. The cigarette smoke was aspirated for 15 sec by the syringe through the cigarette filter and tube A. Then the three-way stopcock was adjusted to open the line between the syringe and tube B. The smoke was puffed for 15 sec by the syringe through tube B to the inhalation cylinder using the same rate of aspiration. Then the process was stopped for 30 sec to complete one cycle. This procedure was repeated till the end of the cigarette burning [10 min][13]. So, smoke puffing occurred for 15 sec. every min simulating the mainstream exposure[1].

Animal studies

Serological Study

Immediately, after the end of the second week, at the Biochemistry Department, Faculty of Medicine, Cairo University, blood samples from the rats of all subgroups were collected from their tail veins to measure cotinine serum level. Cotinine is a nicotine metabolite which is slowly metabolized and excreted by the kidneys. It is used as a marker for tobacco smoke exposure as it has 8-9 times longer half-life than nicotine. In addition, its level remains constant throughout the period of smoke exposure[14].

Animals' sacrifice

At the end of the experimental duration (2 weeks), all the rats of the control subgroups (Ia & IIa) together with the rats of the smoke-exposed subgroups (Ib & IIb) whose blood cotinine level was more than 2.1 ng/ml were sacrificed. This serum cotinine level is the minimal level indicating the rat exposure to SHS[1].

At the laboratory animal house unit, the animals were euthanized by intraperitoneal injection of ketamine (90 mg/kg)/xylazine (15 mg/kg)[15]. The chests were opened, and the lungs of all animals were dissected. The left lung of each animal was divided into 3 equal parts. The first part was used for lung homogenates preparation and quantitative real-time polymerase chain reaction [qRT-PCR], the second part was used to prepare paraffin blocks while the third part was used to prepare resin blocks.

Lung Homogenates and ELISA

Lung homogenates were prepared at Biochemistry Department, Faculty of Medicine, Cairo University, based on a previously described methodology[16]. This was followed by ELISA respecting the manufacturer's instructions and using the suitable antibodies to measure the values of:

- Hydrogen peroxide (H2O2, oxidant agent) [MBS3808898, MyBioSource, USA].
- Nuclear factor kappa-B (NFκ-B, transcription factor for proinflammatory cytokines) [MBS268833, MyBioSource, USA].

Quantitative real-time polymerase chain reaction (qRT-PCR)[16]

It was done at Biochemistry Department, Faculty of Medicine, Cairo University using Rotor Gene 6000 series software version 1.7 (Corbett Life Science, USA) and the primers, to detect the relative mRNA expression of:

- Matrix metalloproteinase-1 (MMP-1 or interstitial collagenase, that breaks down the interstitial collagens I, II & III).
- Matrix metalloproteinase-2 (MMP-2 or gelatinase-A, that breaks down collagen IV of the basement membranes).
- Neutrophil elastase (NE or elastase-2, a neutral serine protease that breaks down the elastic fibers).

This was achieved after extracting the total RNA and synthesizing the complementary DNA. The results were expressed as a normalized ratio.

The used primer PCR sequences were:

- -MMP-1 (forward: 5′-TTGTTGCTGCCCATGAGCTT-3′; reverse: 5′-ACTTTGTCGCCAATTCCAGG -3′).
- -MMP-2 (forward: 5′-GAGATCTGCAAACAGGACAT-3′; reverse: 5′-GGTTCTCCAGCTTCAGGTAA-3′).
- -NE (forward: 5′-GGGGATCCATGGTAGTTGGGGGTCAAGAG-3′; reverse: 5′-GGGAATTCTTAGTTCTTTGCAATCAC-3′).
- -Beta-actin [internal control] (forward: 5′-ACTGCCGCATCCTCTTCCTC-3′; reverse: 5′-ACTCCTGCTTGCTGATCCACAT-3′).

Histological Study

Paraffin block preparation

The lung parts for paraffin block preparation from all animals were fixed in 10% formol saline and kept for 24 hours then processed to paraffin blocks. Six µm-thick sections were cut and stained with:

1. Hematoxylin and Eosin stain (H&E)[17].
2. Orcein stain for elastic fibers[17].
3. Immunohistochemical staining for:
    a. Clara cell secretory protein (CCSP) [rabbit polyclonal antibody, MBS616284, MyBioSource, USA]: it is a specific marker for Clara cells and their secretion that appears as a cytoplasmic reaction.
    b. Surfactant Protein-C (SP-C) [rabbit polyclonal antibody, MBS8291882, MyBioSource, USA]: it is a specific marker for the protein component of the pulmonary surfactant of pneumocytes-II that appears as a cytoplasmic reaction in pneumocytes-II and a reaction on the surface of the alveolar epithelium.
    c. ß-tubulin [rabbit polyclonal antibody, MBS2537225, MyBioSource, USA]: it is a specific marker for surface cilia of the ciliated cells.
    d. Caspase-3 [rabbit polyclonal antibody, MBS628492, MyBioSource, USA]: it is a specific marker for apoptosis that appears as a cytoplasmic reaction in apoptotic cells.
    e. CD-68 [mouse monoclonal antibody, MBS438121, MyBioSource, USA]: it is a marker for macrophages that appears as a cytoplasmic reaction in dust cells.

Immunostaining, using avidin-biotin technique pretreatment[17] was done by boiling the sections for 10 min in 10 mM citrate buffer (cat no 005000) pH 6 for antigen retrieval. Then the sections were left to cool for 20 min at room temperature. This was followed by sections incubation with the primary antibodies for one hour. Ultravision One Detection System (cat no TL - 060-HLJ) was used to complete the immunostaining. Next, counterstaining was performed using Lab Vision Mayer's hematoxylin (cat no TA- 060- MH).

Negative control sections were arranged by the same process after primary antibodies exclusion. Citrate buffer, Ultravision One Detection System and Ultravision Mayer's hematoxylin were purchased from Labvision, ThermoFisher scientific, USA.

Resin block preparation

The lung specimens for resin block preparation from all rats were cut into small pieces (0.5-1.0 mm3). The small fragments were prefixed in 2.5 % glutaraldehyde for 2 h then postfixed in 1% osmium tetroxide in 0.1 M phosphate buffer at pH 7.4 and 4 °C for 2 h. Then, dehydration and resin embedding were carried out.

Semithin (1 µm) and ultrathin (60–90 nm) sections were cut using a Leica ultracut (UCT) (Glienicker, Berlin, Germany). The semithin sections were stained with toluidine blue (1%) and examined by light microscope whereas, ultrathin ones were stained with uranyl acetate followed by lead citrate and examined by transmission electron microscope (TEM) [JEOL JEM-1400, Japan][17].

Morphometric study

It was done by the image analysis using Leica Qwin-500 LTD-software image analysis computer system (Cambridge, England) to measure:

The area percent [in ten non-overlapping fields (×100)] of:

- Elastic fibers surrounding the bronchioles, the airspaces & in the crested septa (not the blood vessels) in sections stained with Orcein stain. This was achieved via subtracting the mean area percent of the elastic fibers that surrounded the blood vessels from that measured in the whole field.
- CCSP, SP-C, ß-tubulin, and caspase-3 immuno-expressions in the corresponding immunostained sections.

The mean number [in ten non-overlapping fields (×100)] of:

- SP-C positive cells in its immunostained sections.
- CD-68 positive cells in its immunostained sections.

Statistical analysis

The morphometric and biochemical measurements were stated as mean ± standard deviation (SD). They were statistically analyzed using one-way analysis of variance (ANOVA) followed by "Tukey" post hoc test. This was carried out using IBM Statistical Package for the Social Sciences (SPSS) version 21 at the Histology Department, Faculty of Medicine, Cairo University. The results were considered statistically significant when *P value* was < 0.05.

All histological studies, morphometric studies and statistical analysis were done at Histology Department, Faculty of Medicine, Cairo University, except the examination of the ultrathin sections. They were done at Electron Microscope Research Unit, Faculty of Agriculture, Cairo University.

RESULTS

General observations

In the rats of the pilot study, the animals revealed marked decrease in their activity with signs of respiratory distress with the start of their exposure to the 2nd cigarette smoke at each exposure time. However, in the experimental animals, no deaths nor abnormal behaviour was observed.

The animals of subgroups (Ia & IIa) were called child-control and adult-control subgroups, respectively.

Animal Data

Serological Results (Figure 2)

Level of cotinine (Figure 2a) was almost absent in child-control and adult-control subgroups (subgroups Ia & IIa), however in subgroup Ib it revealed significant increase when compared to subgroup IIb.

Biochemical results (ELISA & qRT-PCR)

Levels of H2O2 & NFκ-B measured by ELISA (Figure 2b) and MMP-1, MMP-2 & NE relative mRNA expression detected by qRT-PCR (Figure 2c) revealed a significant increase in subgroups Ib & IIb than the control subgroups Ia & IIa, respectively. In addition, subgroup Ib demonstrated significant increase of these levels versus subgroup IIb.

Histological Results

Light microscope examination

H&E and toluidine blue-stained sections

In the control subgroup Ia [child-control] (Figures 3 a–c) & subgroup IIa [adult-control] (Figures 3 d–f), the lung sections appeared with spongy appearance where there were a lot of alveolar spaces. Some of these alveoli were visualized singly while the others were arranged in groups forming either alveolar sacs where clusters of alveoli opened in a common atrium or alveolar ducts that had no bronchiolar walls but successive alveolar openings. The alveoli appeared lined with single layer of alveolar epithelium (pneumocytes-I and pneumocytes-II). The pneumocytes-I (squamous alveolar cells) were flat plate-like cells. They had flat, small nuclei and little cytoplasm. Whereas the pneumocytes-II (great alveolar cells) appeared more common than pneumocytes-I and sometimes present in groups of 2 cells. They were cuboidal cells that bulged inside the alveolar lumen with foamy cytoplasm and large, vesicular nuclei with prominent nucleoli.

In-between the alveoli, there were inter-alveolar septa that revealed a network of multiple capillaries with single layer of endothelial cells. Sometimes, these septa were short and incomplete forming the crested secondary septa (projections from the inter-alveolar septa with dilated ends from which new septa grow). Alveolar macrophages (dust cells) were noted in some of these inter-alveolar walls as large cells with eccentric nuclei and slightly vacuolated cytoplasm with some dark particles.

In child-control sections, the alveoli were smaller than those of adult-control, the septa were thicker, and the crested secondary septa were more numerous.

Among the alveoli, there were different-sized bronchioles. The wall of these bronchioles revealed a single layer of epithelial cells. Outside the epithelial layer, there were a thin layer of CT, a layer of circularly arranged smooth muscle cells then another layer of CT. The bronchiolar epithelium was formed of single layer of cuboidal cells [ciliated and Clara cells] with vesicular nuclei that were denser in Clara cells. The ciliated cells showed apical cilia and apical cytoplasmic basal bodies. However, Clara cells were demonstrated as dome-shaped non-ciliated cells with apical caps bulging into the bronchiolar lumen with granular cytoplasm as well as some cytoplasmic vacuoles.

Lung sections of both the child/smoke-exposed subgroup [subgroup Ib] (Figures 3 g–i) & the adult/smoke-exposed subgroup [subgroup IIb] (Figures 3 j–l) showed inflammatory and cellular degenerative features

which were more prominent in the sections of subgroup Ib than in the sections of subgroup IIb. They demonstrated dilated congested blood vessels, extravasated RBCs, and inflammatory cell infiltration in the apparently thickened inter-alveolar septa and around the bronchioles. Additionally, there was deposition of dark particles in the dispersed dust cells. Moreover, most of the alveolar epithelial cells (pneumocytes I & II) and the bronchiolar epithelial cells (ciliated & Clara cells) demonstrated shrunken deeply stained nuclei, or irregular nuclei. In addition, the ciliated cells showed interruption or partial loss of their cilia. Furthermore, there were areas of lost or separated bronchiolar epithelium.

The alveolar spaces appeared enlarged and dilated with reduced crested secondary septa. Moreover, some bronchiolar and alveolar cells were desquamated inside the bronchiolar and the alveolar lumens.

Orcein stained sections

Elastic fibers in subgroup Ia (Figure 4a) & subgroup IIa (Figure 4b) were detected as sheets of fibers around the pulmonary vasculature and as long tortuous fibers around the bronchioles, around the alveoli and in the crested secondary septa. However, in subgroup Ib (Figure 4c) & subgroup IIb (Fig. 4d) the elastic content, especially around the alveoli, the bronchioles and in the crested septa, appeared reduced, interrupted, and granular instead of being fibrillar.

CCSP immunostained sections

The positive immunoreaction was visualized widely spread among the bronchiolar Clara cells' cytoplasm in subgroups Ia (Figure 5a) and subgroup IIa (Figure 5b). Then, the immunoreaction was reduced among Clara cells in subgroup Ib (Figure 5c) and subgroup IIb (Figure 5d) in addition to its detection in some detached cells in the bronchiolar lumen.

SP-C immunostained sections

Abundant positive immunoreaction was demonstrated in the cytoplasm of pneumocytes-II in addition to some positive reaction on the luminal surface of the alveoli in subgroup Ia (Figure 5f) and subgroup IIa (Figure 5g). The reaction was dramatically decreased in subgroup Ib (Figure 5h) and subgroup IIb (Figure 5i).

B-tubulin immunostained sections

There was widely distributed positive immunoreaction on the apical surface of the bronchiolar ciliated cells in subgroup Ia (Figure 5l) and subgroup IIa (Figure 5m). In subgroup Ib (Figure 5n) and subgroup IIb (Figure 5o), the positive immunoreaction was noted to be diminished and disrupted.

Caspase-3 immunostained sections

The positive cytoplasmic immunoreaction was demonstrated to be minimal in the alveolar and bronchiolar epithelium in subgroup Ia (Figure 6a) and subgroup IIa (Figure 6b), then it showed marked increase in the alveolar, the bronchiolar, the endothelial cells and in some detached cells in the lumens in subgroup Ib (Figures 6 c,d) and subgroup IIb (Figures 6 e,f).

CD-68 immunostained sections

Few positive cytoplasmic immunoreaction was detected in subgroup Ia (Figure 6h) and subgroup IIa (Figure 6i) in the alveolar septa and the alveolar lumens. However, in subgroup Ib (Figure 6j) and IIb (Figure 6k), such cytoplasmic immunoreaction was widely distributed.

Electron microscope examination

Ultra-thin sections

The control subgroups [Ia (Figures 7 a–c) & IIa (Figures 7 d,e)] showed normal ultrastructure details of the lung alveolar epithelial cells (pneumocytes-I & pneumocytes-II). Pneumocytes-I appeared as flat cells with small, oval nuclei and thin cytoplasm with few mitochondria, rough endoplasmic reticulum (rER) and some pinocytic vesicles.

Moreover, pneumocytes-II were joined to pneumocytes-I by cellular junctions. They were dome-shaped cells with apical short microvilli and large vesicular nuclei with prominent nucleoli. Their cytoplasm demonstrated rER, large, rounded mitochondria, and multiple lamellar bodies (vesicles of concentrically arranged lamellae).

The bronchiolar epithelial cells [ciliated and Clara cells] appeared in the sections joined together by cellular junctions. The ciliated cells had oval non-lobed nuclei with prominent nucleoli, some rER and their apical cytoplasm possessed mitochondria and numerous basal bodies from which numerous cilia originated.

However, Clara cells were non-ciliated cells with short wide cell membrane irregularities. They exhibited elongated bilobed nucleus with their arms directed basally. Besides, there were some secretory granules, numerous sER with electron-lucent lumens, abundant rER with narrow cisternae, and a lot of elongated mitochondria.

Some Clara cells revealed apical caps which were apical projections from the cells with very large quantities of sER. Sometimes, these caps were seen completely detached in the bronchiolar lumens.

Sections of subgroup Ib (Figures 8 a–c) and subgroup IIb (Figures 8 d–f) displayed signs of degeneration in the alveolar cells where pneumocytes-I appeared with degenerated mitochondria, dilated rER and chromatin margination. Moreover, there was shrunken nuclei in subgroup Ib. However, pneumocytes-II revealed loss or disruption of their apical microvilli, partial or complete loss of the lamellae in the lamellar bodies, dilated rER and degenerated mitochondria (swollen with disrupted cristae). Their nuclei revealed chromatin margination in both subgroups and shrunken nuclei in subgroup Ib.

Furthermore, the bronchiolar ciliated cells demonstrated interruption or partial loss of cilia, degenerated mitochondria, dilated rER, and shrunken nuclei with marginated chromatin. Additionally, Clara cells showed diminished secretory granules, degenerated mitochondria, widening of sER & rER, and loss of their membrane irregularities (almost flat cell membrane) in subgroup IIb. In addition, there was shrunken dense nuclei with chromatin margination in subgroup Ib.

Morphometric Results

Mean area percent of elastic fibres around the alveoli and the bronchioles, CCSP, SP-C and β-tubulin (Figures 4e,5e,5j,5p) and mean number of SP-C positive cells (Figure 5k) demonstrated a significant decrease in subgroups Ib & IIb versus subgroups Ia & IIa, respectively. Moreover, there was significant decrease in subgroup Ib when compared with subgroup IIb. Conversely, the mean area percent of caspase-3 (Figure 6g) and mean number of CD-68 positive cells (Figure 6l) revealed significant increase in subgroup Ib and subgroup IIb in comparison with subgroup Ia and subgroup IIa, correspondingly. Besides, there was significant increase in subgroup Ib versus subgroup IIb.

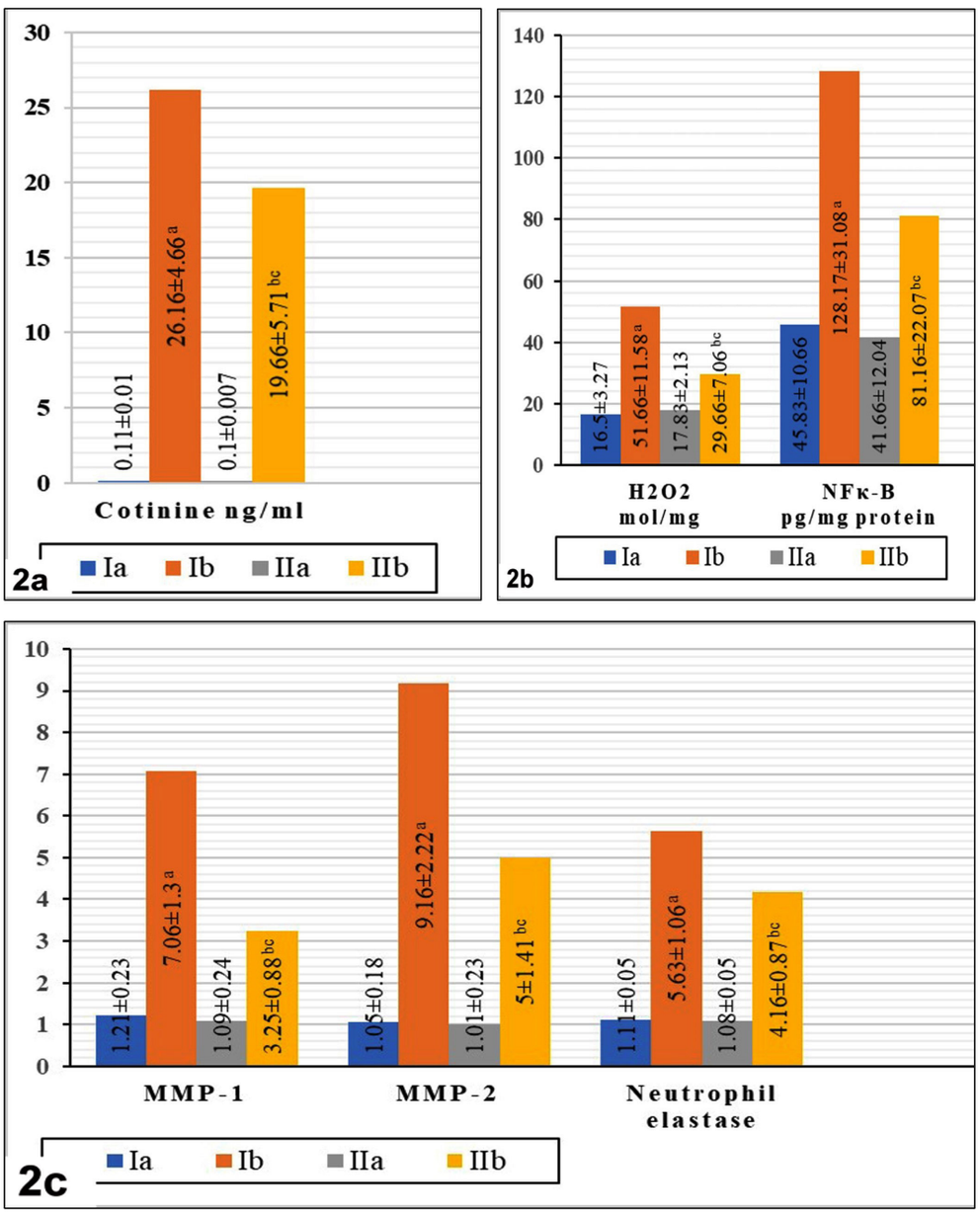

Fig. 2: Showing mean values of: **2a:** Serum cotinine. **2b:** Lung homogenate H2O2 and NFκ-B levels. **2c:** MMP-1, MMP-2 & NE relative mRNA expression. [a, b & c as compared to subgroup Ia, subgroup Ib & subgroup IIa, respectively (significant difference at $P < 0.05$)]

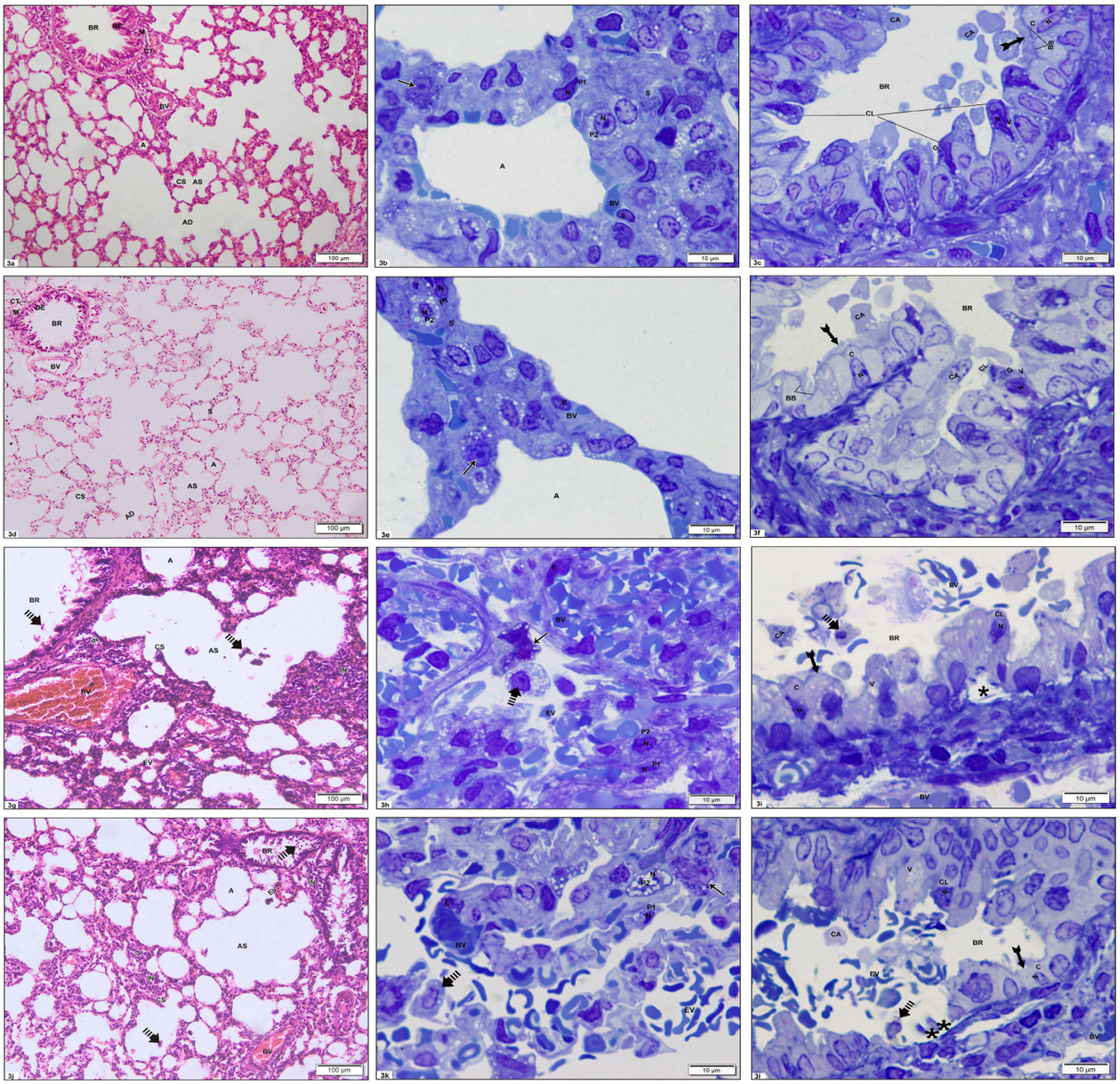

Fig. 3: Photomicrographs of H&E and toluidine blue-stained sections in the lungs of the studied subgroups. [a, b & c: child control, Ia (21 days), d, e & f: adult control, IIa (90 days), g, h & i: child SHS, Ib (21 days) and j, k & l: adult SHS, IIb (90 days)] **3a & 3d (H & E, x100):** Lung alveoli (A) which are smaller in [3a], alveolar sacs (AS) and alveolar ducts (AD) are seen. There are some inter-alveolar septa (S) with network of blood capillaries (BV) which are thicker in [3a]. Short, small inter-alveolar or crested secondary septa (CS) are visualized. A bronchiole (BR) shows single layer of bronchiolar epithelium (BE), thin layer of connective tissue (CT), layer of smooth muscle cells (M) and another layer of connective tissue (CT). **3b & 3e (Toluidine blue, x1000):** Lung alveoli (A) appear lined with Pneumocytes-I (P1) with scanty cytoplasm and small flat nuclei (N) and pneumocytes-II (P2) with foamy cytoplasm and large pale nuclei (N). Inter-alveolar septa (S) with network of blood capillaries (BV) lined with endothelial cells (E) are detected to be thicker in [3b]. Alveolar macrophages are also seen (arrow). **3c & 3f (Toluidine blue, x1000):** A bronchiole (BR) is lined with two types of cells; ciliated (C) and Clara cells (CL). The ciliated cells have vesicular nuclei (N), apical cilia (bifid arrow) and apical dense cytoplasmic bodies referring to the ciliary basal bodies (BB). Dome-shaped, non-ciliated Clara cells appear with vesicular nuclei (N) that are darker than that of the ciliated cells. They also show Clara caps (CA), and granulated cytoplasm (G) with some small cytoplasmic vacuoles (V). **3g & 3j (H & E, x100):** Dilated enlarged alveolar spaces (A) and alveolar sacs (AS) together with relatively few secondary crested septa (CS) projecting in the lumen are seen. Prominent thickened inter-alveolar septa (S) with dilated congested capillaries (BV) are observed. Inflammatory cellular infiltration (IN) in these thick septa and around the bronchiole (BR) can also be observed. Desquamated alveolar & bronchiolar cells (dashed arrow) are noticed in their lumens. In addition, Extravasated RBCs (EV) are recognized. **3h & 3k (Toluidine blue, x1000):** Cellular degenerative and inflammatory features can be visualized such as dilated congested blood vessels (BV) that are lined with endothelial cells (E), extravasated RBCs (EV), dispersed dust cells (arrow), shrunken deeply stained or irregular nuclei (N) in most of pneumocytes-I (P1), II (P2) and desquamated alveolar cells (dashed arrow) inside the alveolar lumens. **3i & 3l (Toluidine blue, x1000)**: A bronchiole (BR) shows separation (*) [3i] or complete loss (**) [3l] of certain areas of the bronchiolar epithelium. Additionally, the two figures demonstrate shrunken deeply stained or irregular nuclei (N) of most of the ciliated (C) & Clara cells (CL), interruption or partial loss of cilia (bifid arrow) in ciliated cells, some vacuolations (V) in Clara cells and desquamated bronchiolar cells (dashed arrow) inside the lumen. Congested blood vessels (BV) and extravasated RBCs (EV) are also seen. Notice the appearance of separated Clara caps (CA) in the lumen.

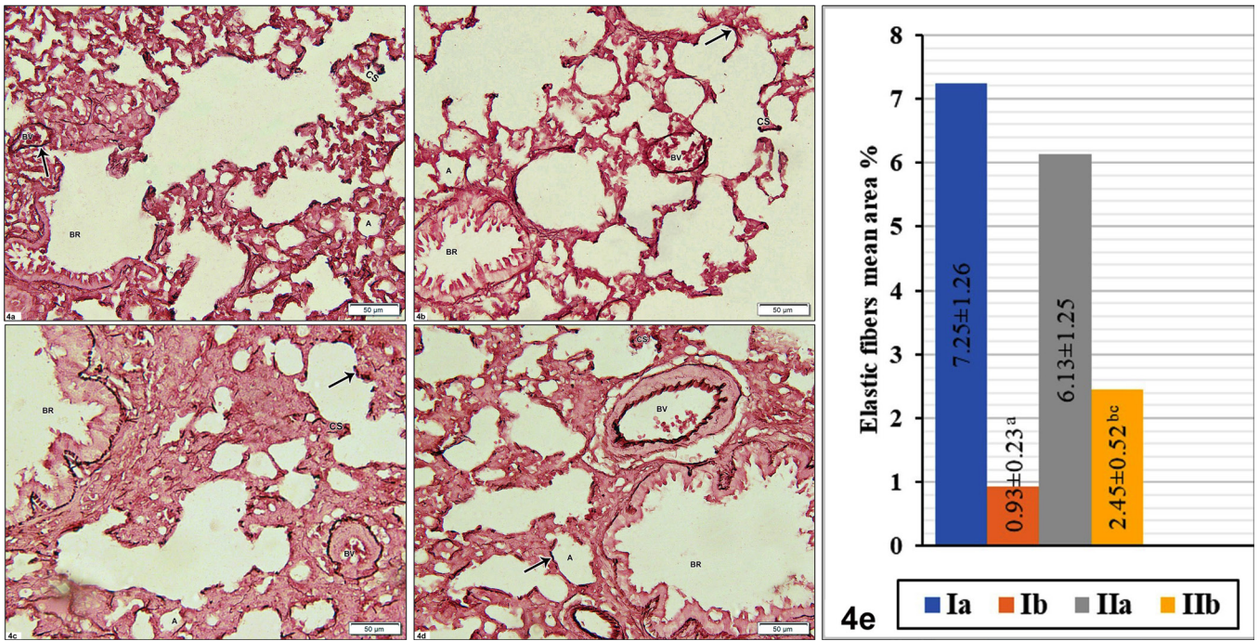

Fig. 4: Photomicrographs of Orcein stained sections in the lungs of different studied subgroups. [a (child control, Ia), b (adult control, IIa), c (child SHS, Ib) and d (adult SHS, IIb)] The arrow indicates positive reaction for elastic fibers. 4a & 4b (Orcein, x200): Long tortuous fibers around the alveoli (A), the bronchioles (BR) and in the crested secondary septa (CS) are seen. In addition, there are sheets of elastic fibers around the blood vessels (BV). 4c & 4d (Orcein, x200): Interrupted, granular elastic fibers around the alveoli (A), the bronchioles (BR) and in the crested septa (CS) are detected. Sheets of elastic fibers with almost normal appearance around the blood vessels (BV) are visualized. 4e: Demonstrating the mean area % of Orcein stained elastic fibers. [a, b & c as compared to subgroup Ia, subgroup Ib & subgroup IIa, respectively (significant difference at $P < 0.05$)]

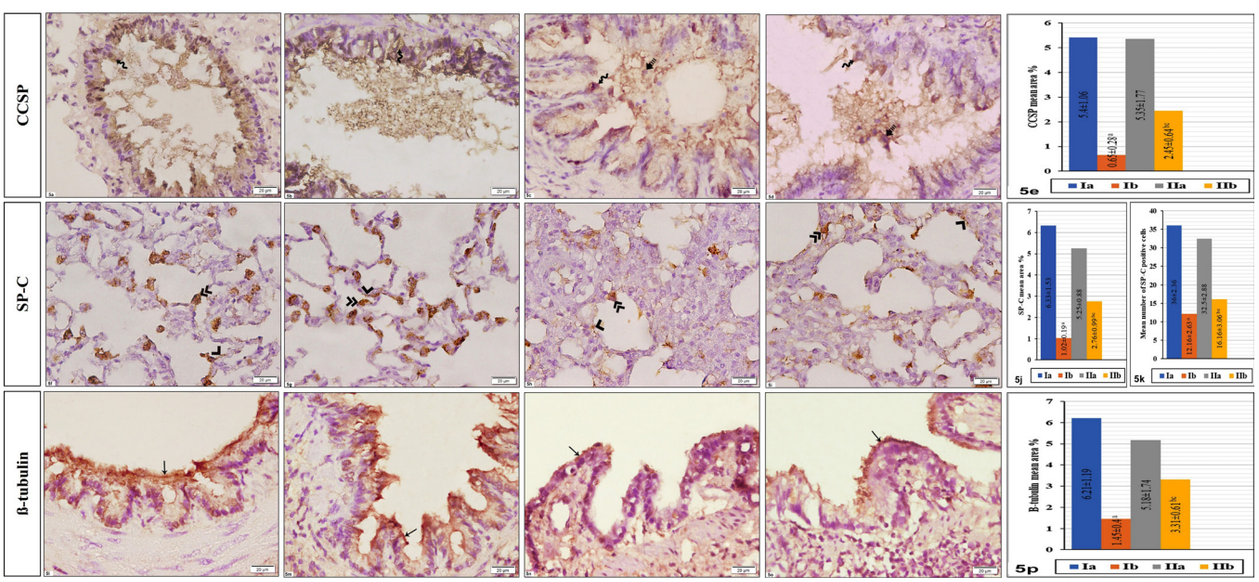

Fig. 5: -Photomicrographs of CCSP immunohistochemically stained sections in the lungs of different studied subgroups. [a (child control, Ia), b (adult control, IIa), c (child SHS, Ib) and d (adult SHS, IIb)] The wavy arrow indicates positive cytoplasmic reaction for Clara cells while the dashed arrow points to detached cell in the bronchiolar lumens. (Immunohistochemical stain for CCSP, x400) 5e: Demonstrating the mean area % of CCSP positive immunoreaction. [a, b & c as compared to subgroup Ia, subgroup Ib & subgroup IIa, respectively (significant difference at **P** < 0.05)] -Photomicrographs of SP-C immunohistochemically stained sections in the lungs of different studied subgroups. [f (child control, Ia), g (adult control, IIa), h (child SHS, Ib) and i (adult SHS, IIb)] The double arrowhead indicates positive cytoplasmic reaction for pneumocytes-II while the arrowhead points to the immunoreaction on the luminal surface of the alveoli. (Immunohistochemical stain for SP-C, x400) 5j & 5k: Demonstrating the mean area % of SP-C positive immunoreaction and the mean number of SP-C positive cells. [a, b & c as compared to subgroup Ia, subgroup Ib & subgroup IIa, respectively (significant difference at $P < 0.05$)] -Photomicrographs of β-tubulin immunohistochemically stained sections in the lungs of different studied subgroups. [l (child control, Ia), m (adult control, IIa), n (child SHS, Ib) and o (adult SHS, IIb)] The arrow indicates positive reaction on the apical surfaces of the bronchiolar ciliated cells. (Immunohistochemical stain for β-tubulin, x400) 5p: Demonstrating the mean area % of β-tubulin positive immunoreaction. [a, b & c as compared to subgroup Ia, subgroup Ib & subgroup IIa, respectively (significant difference at $P < 0.05$)]

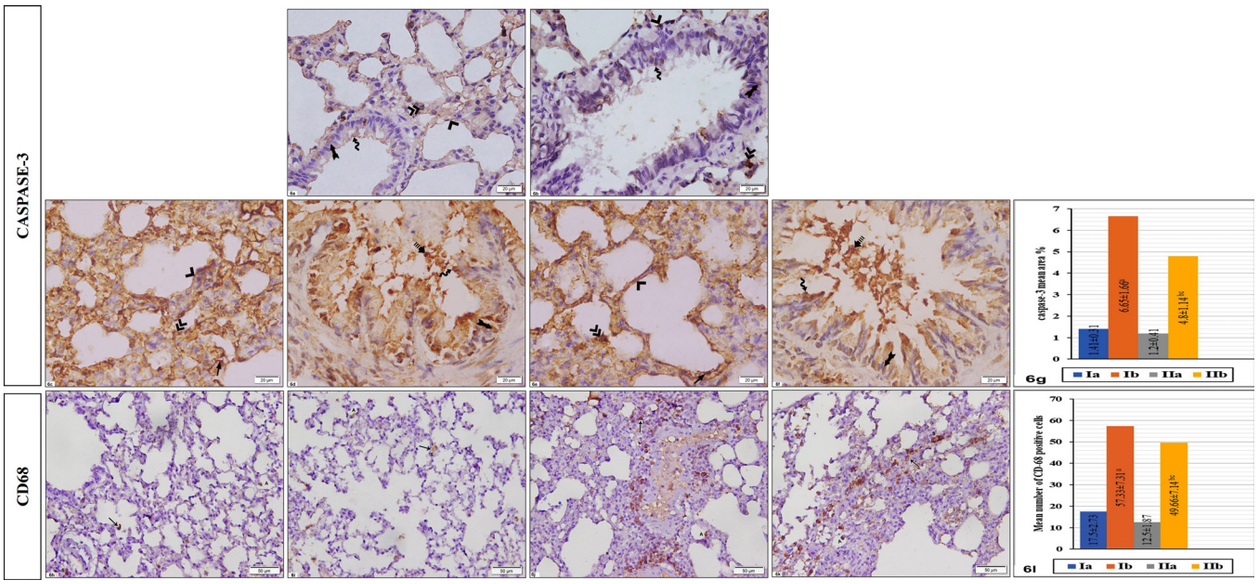

Fig. 6: -Photomicrographs of caspase-3 immunohistochemically stained sections in the lungs of different studied subgroups. [a (child control, Ia), b (adult control, IIa), c & d (child SHS, Ib) and e & f (adult SHS, IIb)] The double arrowhead indicates positive cytoplasmic reaction for pneumocytes-II, the arrowhead points to pneumocytes-I, the wavy arrow reveals the bronchiolar Clara cells, the bifid arrow denotes the bronchiolar ciliated cells, the arrow specifies the endothelial cells while the dashed arrow indicates detached cell in the bronchiolar lumens. (Immunohistochemical stain for caspase-3, x400) 6g: Demonstrating the mean area % of caspase-3 positive immunoreaction. [a, b & c as compared to subgroup Ia, subgroup Ib & subgroup IIa, respectively (significant difference at $P < 0.05$)] -Photomicrographs of CD-68 immunohistochemically stained sections in the lungs of different studied subgroups. [h (child control, Ia), i (adult control, IIa), j (child SHS, Ib) and k (adult SHS, IIb)] The arrow reveals positive cytoplasmic reaction in the inter-alveolar septa (S) & in the alveolar lumens (A). (Immunohistochemical stain for CD-68, x200) 6l: Demonstrating the mean number of CD-68 positive cells. [a, b & c as compared to subgroup Ia, subgroup Ib & subgroup IIa, respectively (significant difference at $P < 0.05$)]

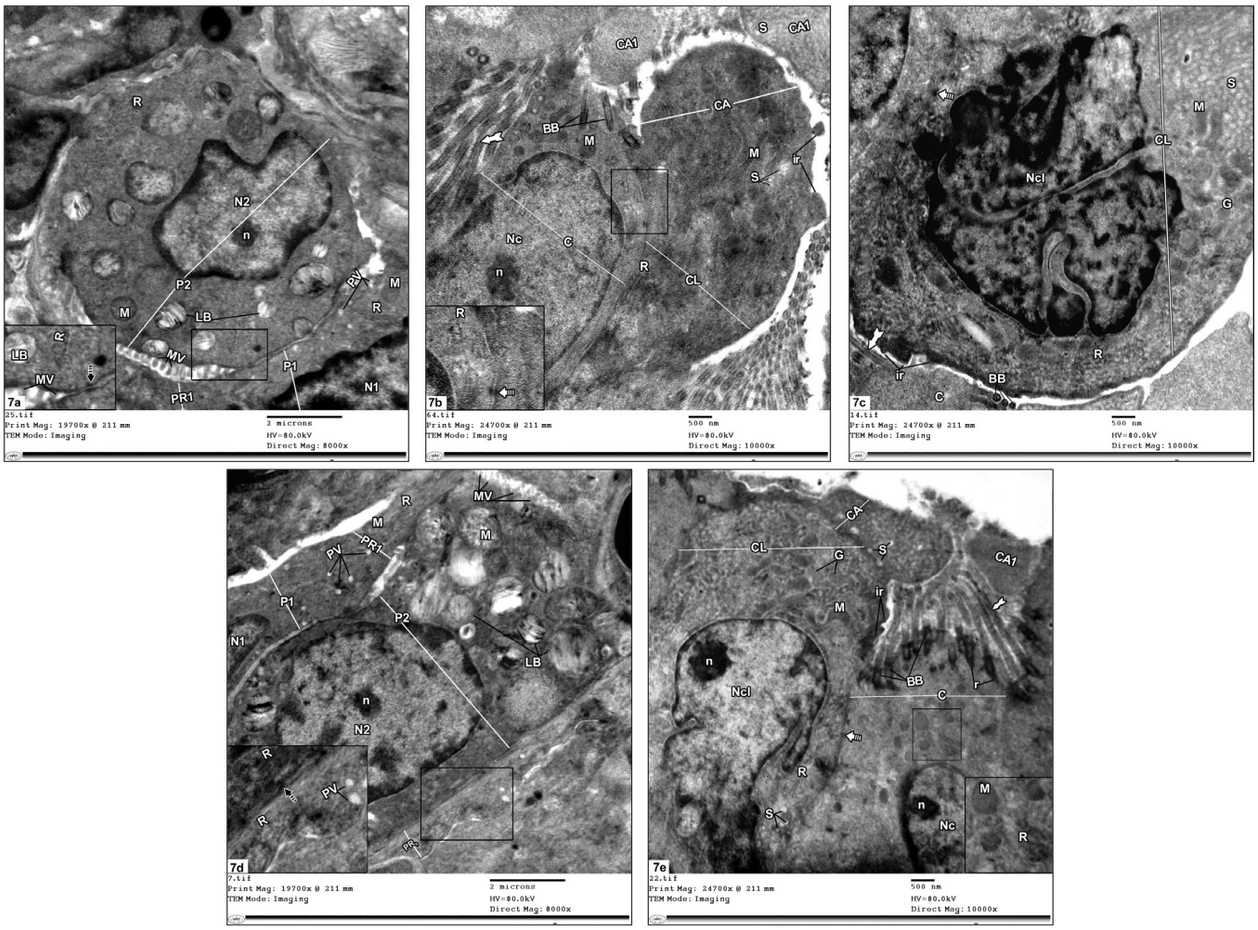

Fig. 7: Transmission electron micrographs of the lungs from the two studied control subgroups. [a, b &c (child control, Ia) and d & e (adult control, IIa)] 7a (Ultra-thin sections, x8000 – inset, x10000): A part of pneumocyte-I (P1) and its process (PR1) are observed with its nucleus (N1), cytoplasm with few rER (R), mitochondria (M) and some pinocytic vesicles (PV). A Pneumocyte-II (P2) reveals apical short microvilli (MV), large euchromatic nucleus (N2) with prominent nucleolus (n), rER (R), large, rounded mitochondria (M) and multiple lamellar bodies (LB). The inset shows part of the pneumocyte-II with rER (R), a lamellar body (LB), apical microvilli (MV) and cell junctions (dashed arrow) with a pneumocyte-I. 7b (Ultra-thin sections, x10000 – inset, x15000): A part of ciliated cell (C) is noticed with oval nucleus (Nc) and prominent nucleolus (n), mitochondria (M) and numerous cilia (bifid arrow) originating from basal bodies (BB). A part of Clara cell (CL) with its apical cap (CA) is demonstrated with short wide cell membrane irregularities (ir), numerous sER (S) with electron-lucent lumens, abundant rER (R) with narrow cisternae and a lot of elongated mitochondria (M). Other Clara caps (CA1) with large quantities of sER are seen completely detached in the bronchiolar lumen. The inset shows part of the ciliated cell with some rER (R) and cell junctions (dashed arrow) with a Clara cell. 7c (Ultra-thin sections, x10000): A Clara cell (CL) is visualized with elongated bilobed nucleus (Ncl) with their arms directed basally, short wide cell membrane irregularities (ir), some secretory granules (G), numerous sER (S) with electron-lucent lumens, abundant rER (R) with narrow cisternae, a lot of elongated mitochondria (M) and cell junctions (dashed arrow) with a ciliated cell. A part of another ciliated cell (C) appears with cilia (bifid arrow) and basal bodies (BB). 7d (Ultra-thin sections, x8000 – inset, x10000): A part of pneumocyte-I (P1) and its process (PR1) are observed with its nucleus (N1), cytoplasm with few rER (R), mitochondria (M) and some pinocytic vesicles (PV). Another pneumocyte-I process (PR1) is detected. A Pneumocyte-II (P2) demonstrates apical short microvilli (MV), large euchromatic nucleus (N2) with prominent nucleolus (n), large, rounded mitochondria (M) and multiple lamellar bodies (LB). The inset demonstrates part of the pneumocyte-II with rER (R) and part of the pneumocyte-I process with rER (R), pinocytic vesicles (PV) and cell junctions (dashed arrow) with a pneumocyte-II. 7e (Ultra-thin sections, x10000 – inset, x15000): A Clara cell (CL) is seen with elongated bilobed nucleus (Ncl) with their arms directed basally & prominent nucleolus (n), short wide cell membrane irregularities (ir), some secretory granules (G), numerous sER (S) with electron-lucent lumens, abundant rER (R) with narrow cisternae, a lot of elongated mitochondria (M), apical cap (CA) with numerous sER (S) and cell junctions (dashed arrow) with a ciliated cell. Another Clara cap (CA1) is seen completely detached in the bronchiolar lumen. The ciliated cell (C) appears with oval nucleus (Nc) and prominent nucleolus (n) and numerous cilia (bifid arrow) originating from basal bodies (BB) with cilia rootlets (r). The inset shows part of the ciliated cell with rER (R) and mitochondria (M).

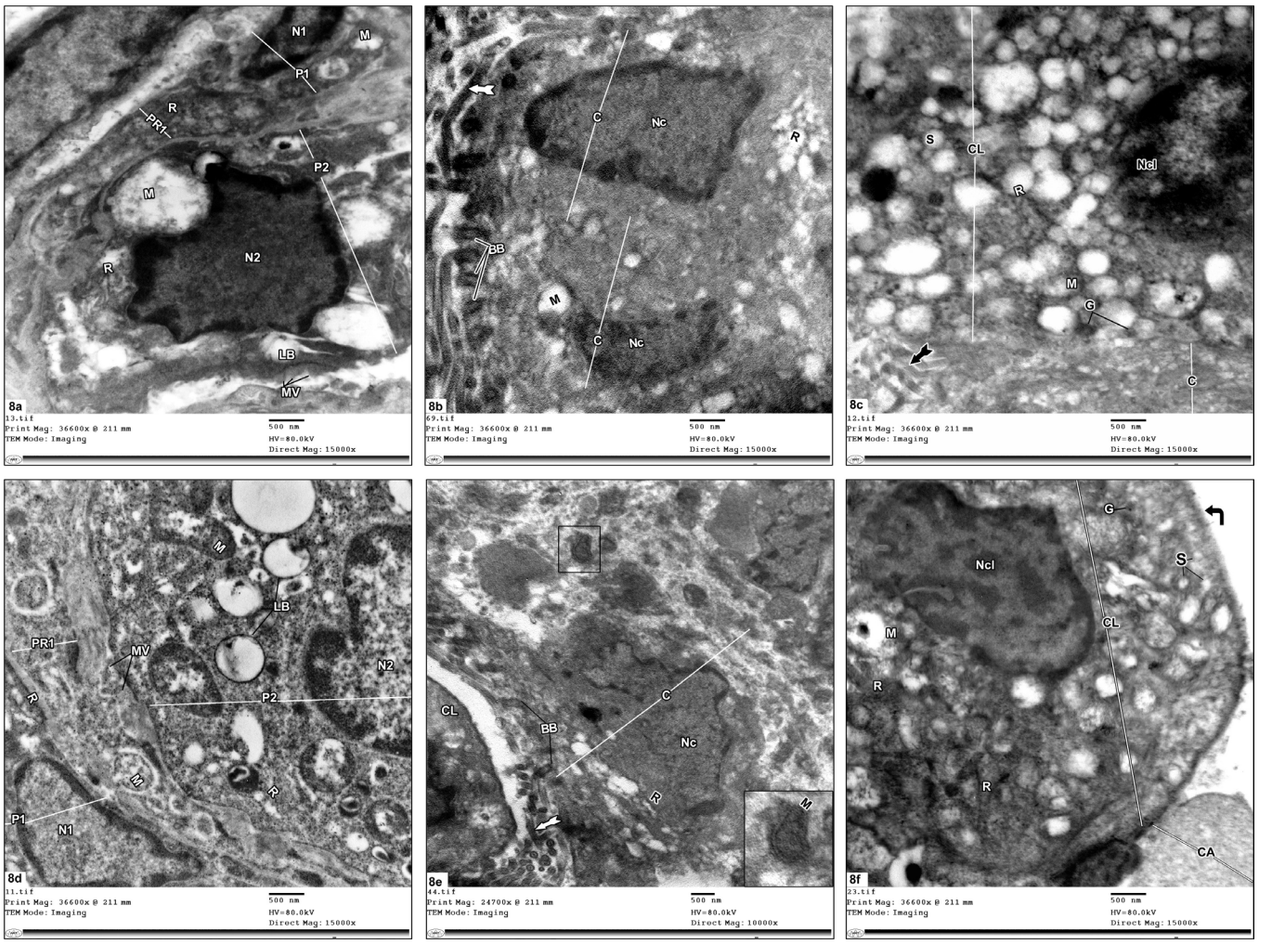

Fig. 8: Transmission electron micrographs of the lungs from the two studied smoke-exposed subgroups. [a, b &c (child SHS, Ib) and d, e & f (adult SHS, IIb)] 8a (Ultra-thin sections, x15000): A part of pneumocyte-I (P1) and its process (PR1) show swollen mitochondria with disrupted cristae (M), dilated rER (R) and degenerated shrunken nucleus (N1) with chromatin margination. Pneumocyte-II (P2) demonstrates degenerated shrunken nucleus (N2) with chromatin margination, swollen mitochondria with disrupted cristae (M), dilated rER (R), lost or disrupted apical microvilli (MV) and partial or complete loss of the lamellae in the lamellar bodies (LB). 8b (Ultra-thin sections, x15000): Two ciliated cells (C) demonstrate shrunken nuclei (Nc) with marginated chromatin, ciliary interruption (bifid arrow) or partial loss of cilia with preserved basal bodies (BB), degenerated mitochondria (M) and dilated rER (R). 8c (Ultra-thin sections, x15000): A Clara cell (CL) is seen with diminished secretory granules (G), degenerated mitochondria (M), widening of sER (S) & rER (R) and shrunken dense nucleus with marginated chromatin (Ncl). A part of ciliated cell (C) with interrupted cilia (bifid arrow) is also seen. 8d (Ultra-thin sections, x15000): A part of pneumocyte-I (P1) and a part of pneumocyte-I process (PR1) show swollen mitochondria with disrupted cristae (M), dilated rER (R) and degenerated nucleus (N1) with chromatin margination. Pneumocyte-II (P2) reveals degenerated nucleus (N2) with chromatin margination, swollen mitochondria with disrupted cristae (M), dilated rER (R), lost or disrupted apical microvilli (MV) and partial or complete loss of the lamellae in the lamellar bodies (LB). 8e (Ultra-thin sections, x10000 – inset, x15000): A ciliated cell (C) reveals shrunken nucleus (Nc) with marginated chromatin, ciliary interruption (bifid arrow) or partial loss of cilia with preserved basal bodies (BB) and dilated rER (R). A part of degenerated Clara cell (CL) is observed. The inset reveals part of the ciliated cell with degenerated mitochondria (M). 8f (Ultra-thin sections, x15000): A Clara cell (CL) appears with reduced secretory granules (G), degenerated mitochondria (M), widening of sER (S) & rER (R), shrunken dense nucleus with marginated chromatin (Ncl) and almost flat cell membrane (right angled arrow). A part of Clara cap (CA) is noted.

DISCUSSION

This study designed to estimate and compare the potential harmful consequences of SHS on the lungs of child and adult male albino rats with underlining the influences on pneumocytes-I & II, bronchiolar ciliated cells, and Clara cells.

Although globally females during their adult life are more exposed to SHS at home and workplaces than males[18], male gender was picked for this work as they are more sensitive to SHS effects than females[19]. This is due to acceleration of cotinine metabolism by female hormones[14]. In addition, the rat's left lung which is formed of one lobe only was chosen to avoid the different histological pictures of the lung lesion in different lobes according to the amount of lobe aeriation and vascularity[20].

The 21st postnatal day (P21) rats were selected for the child-control subgroup as it is the age of childhood beginning[21]. Besides, they are comparable to 3 years human children. In addition, it is the age of finalization of the bulk alveolarization and septal restructuring stages of lung development[22].

The rats' lungs after birth are immature and have air tubules and saccule-like air spaces. Then, they develop very rapidly via two main stages: bulk alveolarization stage [from day 4 to day 13] and late septal restructuring stage [from day 14 to day 21]. During the bulk alveolarization period, there was rapid proliferation of the inter-airspace cells to from two capillary networks with a central thick cellular layer of CT in-between. However, during the late septal restructuring stage, the inter-alveolar septa become mature and formed of a single capillary network with fine supporting CT strands and decreased number of cells. i.e., the lungs have typical structure of the alveoli and interalveolar septa but with smaller alveoli, thicker septa, and numerous crested secondary septa[22].

After that, the mature lung enters the stage of equilibrated growth where there is increase in the size and number of alveoli, thinning of the inter-alveolar septa and increase in the lung volume. So, P90 (90th postnatal day) rats were chosen for the adult-control subgroup as they have fully developed lungs[22] and are stated to be mature adults[21].

In the pilot study, the exposure of the rats (child & adult) to SHS of 2 cigarettes at each time, according to a previous study[1], resulted in respiratory distress. So, the number of cigarettes were reduced to one only at each time of exposure.

In this work, SHS exposure in subgroups Ib and IIb led to a lot of degenerative changes in the interstitium and in the bronchiolar and alveolar cells. Such exposure was documented by the high cotinine serum level in these two subgroups and its almost absence in the control subgroups (Ia & IIa). However, this level was greatly higher than the minimal accepted value for rat SHS exposure [2.1 - 17.5 ng/ml][1]. Such finding could be explained by the rats' exposure to the whole volume of the mainstream smoke not only 1 - 43% of exhaled part as in cases of the usual human SHS exposure where the mainstream smoke is diluted by the environmental air[23].

There are about 7000 components in the cigarette smoke[24] either in gaseous state or solid state. SHS contains all these components but in smaller concentrations[23]. Most of these components were reported to be exogenous oxidants. In addition, the cigarette smoke induces a lot of endogenous oxidants where it stimulates the production of more oxidative agents like reactive oxygen species (ROS) and H2O2 by alveolar macrophages, pneumocytes-II and bronchiolar epithelium mitochondria[25].

So, it was hypothesized in this work that the initial step of the detected SHS effects was oxidative stress due to oxidant/antioxidant imbalance. This was reinforced by the significant increase in the lung homogenate level of H2O2 in the smoke-exposed subgroups versus the control subgroups. This finding is in line with that documented previously[26] following SHS exposure. Further support came from the significant decrease of pulmonary GSH level in a former study after SHS exposure[27].

The smoke-exposed subgroups demonstrated significant increase in homogenate NFκ-B level when compared with the control subgroups. Besides, there were other signs of inflammation (dilated congested blood vessels and inflammatory cell infiltration). All these findings could be explained by OS.

Oxidative stress was known to increase the gene expression of NFκ-B and pro-inflammatory cytokines and chemokines [IL-8, TNF-α and granulocyte-macrophage colony stimulating factor (GMCSF)][25]. Additionally, the cigarette smoke itself activates NFκ-B in the dust and epithelial cells causing its nuclear translocation with further increase in the gene expression of the pro-inflammatory mediators[28]. Finally, this consequential inflammation was recorded to induce more OS creating a viscous circle[25].

The pro-inflammatory mediators, specifically IL-8, were reported previously[29] to augment neutrophil recruitment. Such effect was proved in subgroups Ib and IIb by the significant increase in the NE level (an elastase secreted by neutrophils and considered as a specific marker for these cells[30]) compared to subgroups Ia and IIa. Moreover, TNF-α and GMCSF attract more leucocytes and macrophages and OS itself stimulates phagocytic activity[25]. This was supported by the noticed increase in the number of dust cells and their load with carbon particles.

Interruption of the tight junctions between the epithelial cells and increasing their permeability was proved to occur due to one of the smoke components, namely cadmium[31]. This finding was detected in the current study by the extravasated RBCs resulted from increased endothelial permeability and blood vessels congestion.

SHS-induced cellular degeneration in the smoke-exposed subgroups was followed by apoptotic cell death in all epithelial cells (bronchiolar, alveolar, and endothelial cells). Such apoptosis was recognized by its signs, the presence of desquamated cells inside the bronchioles and the alveoli and the significant increase in the mean area percent of caspase-3 immunoreaction in these two subgroups compared with the control subgroups. Apoptosis was suggested to occur through extrinsic and intrinsic pathways. The extrinsic pathway occurred through stimulation of apoptosis surface receptors, like TNF-α receptors, by the high TNF-α level[32]. While the intrinsic pathway arose from the mitochondrial degeneration documented in this study with consequent production of cytochrome-C. Both pathways result into cascade activation of caspases till reaching caspase-3 with subsequent apoptotic cell death[33].

Although SHS exposure throughout this experimental duration resulted into severe degenerative, oxidative, and inflammatory effects, it did not induce pulmonary fibrosis or alveolar collapse. Astonishingly, it produced emphysematous dilatation and enlargement of the alveoli. This observation was presumed to be due to destruction of the inter-alveolar septa and reduction of the crested secondary septa as a result of the detected secondary apoptosis of the alveolar epithelial and the endothelial cells.

Moreover, the significant increase in the proteases (MMP-1 and MMP-2) homogenate levels following SHS exposure in comparison with the control status could degrade different collagen types in the inter-alveolar septa. These proteases together with others (MMP-9 and MMP-12) were reported to be produced by the alveolar macrophages, the inflammatory cells, and the epithelial cells in response to high levels of proinflammatory cytokines and the cigarette smoke itself[25].

Another assumption for such septal degradation was the elastase/anti-elastase imbalance. This assumption was supported by the detected damage and interruption of elastic fibers. Further support was achieved by the significant increase in the homogenate level of NE (a major elastase produced by neutrophils). Moreover, OS was reported to elucidate marked reduction in the level of alpha-1 antitrypsin (AAT), a major anti-elastase acts mainly against NE[34].

SHS exposure in this work resulted into significant diminution of the mean area percent of Clara cell secretory protein (CCSP), surfactant protein-C (SP-C) & β-tubulin and the mean number of SP-C positive cells, when compared to the control subgroups. These findings were believed to be due to apoptosis of some of Clara cells, pneumocytes-II and ciliated cells along with reduction of the remaining cells' functions by SHS-induced degeneration and OS.

Reinforcement for such functional alteration developed from the recognition of mitochondrial degeneration, dilatation of rER and widening of sER in these cells. In addition, Clara cells revealed loss of their membrane irregularities and decrease or complete loss of their granules with subsequent decrease in their secretion (CCSP). Ciliated cells demonstrated disruption and loss of the cilia. Additionally, pneumocytes-II showed loss of their microvilli together with partial or complete loss of the lamellae of the multilamellar bodies that led to significant decrease in surfactant formation and secretion (SP-C).

Moreover, ciliary dysfunction was reported in a former study[35] following exposure of cultured bronchiolar epithelial cells to mainstream smoke. Furthermore, mucous over-production was also noticed previously to be due to over-stimulation of epidermal growth factor receptor (EGFR) by OS[36] or over-production of transforming growth factor-α (TGF-α) by NE[37]. This was supported in this study by the documented high level of NE in smoke-exposed subgroups. Both ciliary dysfunction and/or over-production of mucous were added to the desquamated epithelial cells to produce the partial obstruction of the bronchioles and the alveoli observed as a sequel to SHS in this work.

These functional alterations together with the decreased gas exchange surface caused by the reported inflammatory infiltration, emphysema and apoptosis of both endothelial cells and pneumocytes-I were assumed to hinder the pulmonary functions. This assumption was confirmed previously[38] where SHS-induced reduction in the pulmonary functions such as forced vital capacity (FVC), forced expiratory volume in one second (FEV1), FEV1/FVC ratio, peak expiratory flow (PEF) and forced expiratory flow (FEF). This, in turn, increases the risk of development of multiple lung diseases like chronic bronchitis, chronic obstructive pulmonary disease (COPD), bronchial asthma and lung cancer[39].

It was of great importance to notice that all SHS-pulmonary histological, and biochemical effects were more pronounced in children than in adults. This observation could be explained by the prolonged accumulation of the smoke components and their metabolites in the children than in the adults[40]. Such explanation was supported by the significant increase in the serum cotinine level in subgroup Ib when compared to subgroup IIb. This marked metabolite accumulation could be illuminated by the lower ability of children to detoxify different metabolites due to immaturity of their enzymes and their clearance systems[41]. Moreover, children are exposed to more SHS than adults as they have higher respiratory rate and breathe more air than adults[42], most probably due to their less developed lungs (small number of alveoli and thick septa).

The more aggressive SHS hazardous effects in children[40] was expected to be followed by marked worsening of the pulmonary functions, more morbidities such as bronchiolitis, pneumonia, wheezes, asthma with higher incidence of hospitalization and more mortalities[43].

From this study, it could be concluded that SHS has marked deleterious effects on the lung histology and

biochemistry in both children and adults. These effects are initiated by OS and completed by inflammatory and apoptotic sequalae. Such sequence is associated with marked diminution of the pulmonary functions because of the degenerative changes in the bronchiolar epithelium (ciliated and Clara cells), the alveolar epithelium (pneumocytes-I and II), and the inter-alveolar septa. Additionally, the children could be considered a very high-risk age group during SHS exposure as they show more damaging effects than adults. Besides, they are more vulnerable to SHS exposure from their parents and guardians at home.

CONFLICT OF INTERESTS

There are no conflicts of interest.

REFERENCES

1. Rosa RC, Pereira SC, Cardoso FA, Caetano AG, de Santiago HA, Volpon JB. Second hand tobacco smoke adversely affects the bone of immature rats. Clinics. 2017; 72:785-9. doi: 10.6061/clinics/2017(12)11
2. Jha P. Avoidable deaths from smoking: a global perspective. Public Health Reviews. 2012; 33:569-600. doi.org/10.1007/BF03391651
3. GBD 2017 Risk Factor Collaborators. Global, regional, and national comparative risk assessment of 84 behavioural, environmental and occupational, and metabolic risks or clusters of risks for 195 countries and territories, 1990–2017: a systematic analysis for the Global Burden of Disease Study 2017. Lancet 2018; 392: 1923–94. doi: 10.1016/S0140-6736(18)32225-6.
4. Prabhat Jha, Richard Peto. Global Effects of Smoking, of Quitting, and of Taxing Tobacco. N Engl J Med. 2014; 370:60-8. doi: 10.1056/NEJMra1308383.
5. Cohen A, George O. Animal models of nicotine exposure: relevance to second-hand smoking, electronic cigarette use, and compulsive smoking. Front Psychiatry. 2013; 4:41. doi: 10.3389/fpsyt.2013.00041.
6. Cheng W, Zhou R, Feng Y, Wang Y. Mainstream smoke and sidestream smoke affect the cardiac differentiation of mouse embryonic stem cells discriminately. Toxicology. 2016; 357-8:1-10. doi: 10.1016/j.tox.2016.05.017.
7. Schick S, Glantz S. Philip Morris toxicological experiments with fresh sidestream smoke: more toxic than mainstream smoke. Tob Control. 2005; 14:396-404. doi: 10.1136/tc.2005.011288.
8. Vasconcelos TB, Araújo FY, Pinho JP, Soares PM, Bastos VP. Effects of passive inhalation of cigarette smoke on structural and functional parameters in the respiratory system of guinea pigs. J Bras Pneumol. 2016; 42:333-40. doi: 10.1590/S1806-37562015000000342.
9. Jacob P 3rd, Benowitz NL, Destaillats H, Gundel L, Hang B, Martins-Green M, Matt GE, Quintana PJ, Samet JM, Schick SF, Talbot P, Aquilina NJ, Hovell MF, Mao JH, Whitehead TP. Thirdhand Smoke: New Evidence, Challenges, and Future Directions. Chem Res Toxicol. 2017; 30:270-294. doi: 10.1021/acs.chemrestox.6b00343.
10. Tan CE, Glantz SA. Association between smoke-free legislation and hospitalizations for cardiac, cerebrovascular, and respiratory diseases: a meta-analysis. Circulation. 2012; 126:2177-83. doi: 10.1161/CIRCULATIONAHA.112.121301.
11. Mbulo L, Palipudi K M, Andes L, Asma S, Sinha D, Ratsimbazafy R R, Rarick J, Caixeta R D B, Khoury R. Secondhand Smoke Exposure among 3.2 Billion Children in 20 Countries. International Journal of Epidemiology. 2015; 44: 32-3. doi: 10.1093/ije/dyv097.107
12. WHO Report on the Global Tobacco Epidemic, 2019: The MPOWER package. Geneva: World Health Organization; 2019. Retrieved from https://www.drugsandalcohol.ie/30850/
13. Brito MVH, Yasojima EY, Silveira EL, Yamaki VN, Teixeira RKC, Feijó DH, Gonçalves TB. New experimental model of exposure to environmental tobacco smoke. Acta Cir Bras. 2013; 28:815-9. doi: 10.1590/s0102-86502013001200002.
14. Benowitz NL, Hukkanen J, Jacob P 3rd. Nicotine chemistry, metabolism, kinetics, and biomarkers. Handb Exp Pharmacol. 2009; 192:29-60. doi: 10.1007/978-3-540-69248-5_2.
15. El-Akabawy G, El-Kholy W. Neuroprotective effect of ginger in the brain of streprozotocin-induced diabetic rats. Ann Anat 2014; 196: 119- 28. doi: 10.1016/j.aanat.2014.01.003.
16. El Agaty SM. Cardioprotective effect of vitamin D2 on isoproterenol-induced myocardial infarction in diabetic rats. Archives of Physiology and Biochemistry. 2019; 125:210-9. doi: 10.1080/13813455.2018.1448423.
17. Suvarna K, Layton C, Bancroft J. The hematoxylins and eosin, Connective, and other mesenchymal tissues with their stains, Immunohistochemical techniques & Transmission electron microscopy. In Bancroft's Theory and Practice of Histological Techniques (Eighth Edition), Elsevier,2019, pp: 126-38, 153-75, 337-94, 434-75. doi: 10.1016/B978-0-7020-6864-5.00010-4.
18. Oberg M, Jaakkola MS, Woodward A, Peruga A, Prüss-Ustün A. Worldwide burden of disease from exposure to second-hand smoke: A retrospective analysis of data from 192 countries. Lancet. 2011; 377:139-46. doi: 10.1016/S0140-6736(10)61388-8.

19. Noël A, Xiao R, Perveen Z, Zaman H, Le Donne V, Penn A. Sex-specific lung functional changes in adult mice exposed only to second-hand smoke in utero. Respir Res. 2017; 18:104. doi: 10.1186/s12931-017-0591-0.

20. Nemec SF, Bankier AA, Eisenberg RL. Upper lobe-predominant diseases of the lung. AJR Am J Roentgenol. 2013; 200: W222-W37. doi: 10.2214/AJR.12.8961.

21. Sengupta P. The Laboratory Rat: Relating Its Age with Human's. Int J Prev Med. 2013; 4:624-30. PMID: 23930179; PMCID: PMC3733029.

22. Tschanz SA, Salm LA, Roth-Kleiner M, Barré SF, Burri PH, Schittny JC. Rat lungs show a biphasic formation of new alveoli during postnatal development. J Appl Physiol (1985). 2014; 117:89-95. doi: 10.1152/japplphysiol.01355.2013.

23. IARC Working Group on the Evaluation of Carcinogenic Risks to Humans. Tobacco smoke and involuntary smoking. IARC Monogr Eval Carcinog Risks Hum. 2004; 83:1-1438. https://www.ncbi.nlm.nih.gov/books/NBK316407/. Retrieved from https://publications.iarc.fr/Book-And-Report-Series/Iarc-Monographs-On-The-Identification-Of-Carcinogenic-Hazards-To-Humans/Tobacco-Smoke-And-Involuntary-Smoking-2004

24. Soleimani F, Dobaradaran S, De-la-Torre GE, Schmidt TC, Saeedi R. Content of toxic components of cigarette, cigarette smoke vs cigarette butts: A comprehensive systematic review. Sci Total Environ. 2022; 813:152667. doi: 10.1016/j.scitotenv.2021.152667.

25. Zuo L, He F, Sergakis GG, Koozehchian MS, Stimpfl JN, Rong Y, Diaz PT, Best TM. Interrelated role of cigarette smoking, oxidative stress, and immune response in COPD and corresponding treatments. Am J Physiol Lung Cell Mol Physiol. 2014; 307: L205-L18. doi: 10.1152/ajplung.00330.2013.

26. Groner JA, Huang H, Eastman N, Lewis L, Joshi MS, Schanbacher BL, Nicholson L, Bauer JA. Oxidative Stress in Youth and Adolescents with Elevated Body Mass Index Exposed to Secondhand Smoke. Nicotine Tob Res. 2016; 18:1622-17. doi: 10.1093/ntr/ntw025.

27. Ycicek A, Erel O, Kocyigit A. Decreased total antioxidant capacity and increased oxidative stress in passive smoker infants and their mothers. Pediatr Int. 2005; 47:635-9. doi: 10.1111/j.1442-200x.2005.02137.x.

28. Zhang C, Qin S, Qin L, Liu L, Sun W, Li X, Li N, Wu R, Wang X. Cigarette smoke extract-induced p120-mediated NF-κB activation in human epithelial cells is dependent on the RhoA/ROCK pathway. Sci Rep. 2016; 6:23131. doi: 10.1038/srep23131.

29. Lee KH, Lee J, Jeong J, Woo J, Lee CH, Yoo CG. Cigarette smoke extract enhances neutrophil elastase-induced IL-8 production via proteinase-activated receptor-2 upregulation in human bronchial epithelial cells. Exp Mol Med. 2018; 50:1-9. doi: 10.1038/s12276-018-0114-1.

30. Lillehoj EP, Kato K, Lu W, Kim KC. Cellular and molecular biology of airway mucins. Int Rev Cell Mol Biol. 2013; 303:139-202. doi: 10.1016/B978-0-12-407697-6.00004-0.

31. Cao X, Lin H, Muskhelishvili L, Latendresse J, Richter P, Heflich RH. Tight junction disruption by cadmium in an in *vitro* human airway tissue model. Respir Res. 2015; 16:30. doi: 10.1186/s12931-015-0191-9.

32. Kokolakis G, Sabat R, Krüger-Krasagakis S, Eberle J. Ambivalent Effects of Tumor Necrosis Factor Alpha on Apoptosis of Malignant and Normal Human Keratinocytes. Skin Pharmacol Physiol. 2021; 34:94-102. doi: 10.1159/000513725.

33. Wu CC, Bratton SB. Regulation of the intrinsic apoptosis pathway by reactive oxygen species. Antioxid Redox Signal. 2013; 19:546-58. doi: 10.1089/ars.2012.4905.

34. Topic A, Milovanovic V, Lazic Z, Ivosevic A, Radojkovic D. Oxidized Alpha-1-Antitrypsin as a Potential Biomarker Associated with Onset and Severity of Chronic Obstructive Pulmonary Disease in Adult Population. COPD. 2018; 15:472-8. doi: 10.1080/15412555.2018.1541448.

35. Aufderheide M, Scheffler S, Ito S, Ishikawa S, Emura M. Ciliatoxicity in human primary bronchiolar epithelial cells after repeated exposure at the air-liquid interface with native mainstream smoke of K3R4F cigarettes with and without charcoal filter. Exp Toxicol Pathol. 2015; 67:407-11. doi: 10.1016/j.etp.2015.04.006.

36. Ning Y, Shang Y, Huang H, Zhang J, Dong Y, Xu W, Li Q. Attenuation of cigarette smoke-induced airway mucus production by hydrogen-rich saline in rats. PLoS One. 2013; 8: e83429. doi: 10.1371/journal.pone.0083429.

37. Nawa M, Osada S, Morimitsu K, Nonaka K, Futamura M, Kawaguchi Y, Yoshida K. Growth effect of neutrophil elastase on breast cancer: favorable action of sivelestat and application to anti-HER2 therapy. Anticancer Res. 2012; 32:13-9. PMID: 22213283. Retrieved from https://ar.iiarjournals.org/content/32/1/13

38. Parro J, Aceituno P, Droppelmann A, Mesías S, Muñoz C, Marchetti N, Iglesias V. Secondhand tobacco smoke exposure and pulmonary function: a cross-sectional study among non-smoking employees of bar and restaurants in Santiago, Chile. BMJ Open. 2017;7: e017811. doi: 10.1136/bmjopen-2017-017811.

39. Goldklang MP, Marks SM, D'Armiento JM. Second hand smoke and COPD: lessons from animal studies. Front Physiol. 2013; 4:30. doi: 10.3389/fphys.2013.00030.

40. Chao MR, Cooke MS, Kuo CY, Pan CH, Liu HH, Yang HJ, Chen SC, Chiang YC, Hu CW. Children are particularly vulnerable to environmental tobacco smoke exposure: Evidence from biomarkers of tobacco-specific nitrosamines, and oxidative stress. Environ Int. 2018; 120:238-45. doi: 10.1016/j.envint.2018.08.006.

41. Ginsberg G, Hattis D, Sonawane B, Russ A, Banati P, Kozlak M, Smolenski S, Goble R. Evaluation of child/adult pharmacokinetic differences from a database derived from the therapeutic drug literature. Toxicol Sci. 2002; 66:185-200. doi: 10.1093/toxsci/66.2.185.

42. Cheraghi M, Salvi S. Environmental tobacco smoke (ETS) and respiratory health in children. Eur J Pediatr. 2009; 168:897-905. doi: 10.1007/s00431-009-0967-3.

43. Hwang SH, Hwang JH, Moon JS, Lee DH. Environmental tobacco smoke and children's health. Korean J Pediatr. 2012; 55:35-41. doi: 10.3345/kjp.2012.55.2.35

الملخص العربى

عواقب التدخين السلبي على رئات ذكور الجرذان البيضاء أثناء فترة الطفولة و فترة البلوغ مع الإشارة بالأخص إلى الخلايا الشعيبية وخلايا الحويصلات

عبير ابراهيم عمر، ايمان عباس فرج، مروة محمد يسري

قسم علم الأنسجة - كلية الطب - جامعة القاهرة – القاهرة – مصر

الخلفية: تدخين التبغ هو أحد الأوبئة الرئيسية ، وهو عامل مهيئ رئيسي للعديد من الأمراض غير المعدية مثل أمراض الأوعية الدموية والقلب والجهاز التنفسي ، وثاني عامل خطر رئيسي للوفاة. يعتبر استنشاق دخان التبغ السلبي والمعروف باسم التدخين السلبي أو دخان التبغ البيئي ، أكثر شيوعًا في البيئة المغلقة (التعرض الداخلي). يتسبب هذا النوع من استنشاق الدخان في ١٥٪ من الوفيات الناجمة عن التدخين و ٢٪ من إجمالي الوفيات. لذلك ، يحظر التدخين في العديد من البلدان في الأماكن العامة المغلقة. في البلدان المنخفضة والمتوسطة اجتماعيا واقتصاديا يكون الأطفال هم أكثر الفئات العمرية المعرضة في منازلهم لخطر التعرض للتدخين السلبي.

هدف العمل: هدفت هذه الدراسة إلى تقييم ومقارنة الآثار الخطرة المحتملة للتدخين السلبي على رئات ذكور الجرذان البيضاء في فترة الطفولة و فترة البلوغ مع تسليط الضوء على عواقبه على الخلايا الشعيبية الهدبية وخلايا كلارا وخلايا الحويصلات -١ و-٢.

المواد وطرق البحث: تم اختيار ٢٤ من ذكور الجرذ ان البيضاء وتقسيمها بالتساوي إلى مجموعة الأطفال (٢١يوم تقريبا، المجموعة الأولى) والمجموعة البالغة (٩٠يوم تقريبا، المجموعة الثانية). تم تقسيم كل مجموعة بالتساوي إلى مجموعتين فرعيتين: التعرض الصوري (تعرضت للهواء النقي ، مرتين يوميًا بفاصل ٦ ساعات) ، والتعرض للدخان (عولجت مثل مجموعة التعرض الصوري الفرعية ولكن باستخدام دخان التبغ السلبي بدلاً من الهواء النقي) . تم قياس مستوى الكوتينين في الدم لجميع الحيوانات بعد أسبوعين قبل التضحية مباشرة. تم إجراء الدراسات الكيميائية الحيوية والنسيجية والهستوكيميائية المناعية] لبروتين إفراز خلايا كلارا، وبروتين الخافض للتوتر السطحي س، وبيتا-توبيولين ، وكاسبيز-٣، و سي دي -٦٨ [والدراسات المترية الشكلية.

النتائج: أظهرت المجموعات الفرعية التي تعرضت للدخان (الأطفال والبالغة) علامات التهابية في الرئة وتغيرات تنكسية في الخلايا الشعيبية الهدبية وخلايا كلارا وفي خلايا الحويصلات -١ و-٢ ، والتي كانت أكثر وضوحًا في مجموعة الأطفال الفرعية.

الاستنتاج:: التدخين السلبي له تأثيرات ضارة شديدة على بنية و وظيفة رئات الجرذان عن طريق آليات الأكسدة ، والالتهابات، وموت الخلايا المبرمج. علاوة على ذلك، فإن الأطفال أكثر عرضة من البالغين لهذه الآثار الضارة.